The Combined Effect of Various Receiver Nonlinearities on Spectrum Sensing in Cognitive Radio Systems

Khaled M. Gharaibeh
College of Engineering, Applied Science University-Bahrain, Manama, Kingdom of Bahrain
Email: khaled.gharaibeh@asu.edu.bh

***Abstract*--**Cognitive Radio (CR) systems which employ Direct Conversion Receivers (DCR) are susceptible to nonlinearities in the receiver path, especially when strong interferes exist. This paper aims to model the combined effect of RF nonlinearities, baseband nonlinearities and I/Q imbalances in wideband CR receivers when strong interferers exist. The analysis presented in this paper is based on considering a cascade of memoryless nonlinearities that model RF nonlinearity, BB nonlinearity and IQ imbalance and an input that consists of a desired and interfering signals. The combined output of the cascade is calculated and nonlinear distortion is identified and related to spectrum sensitivity. The analysis is verified by simulation results which show that nonlinear distortion from the interaction of multiple signals by the RF nonlinearity is significantly enhanced when other BB nonlinearities exist in the receiver path. The simulations also enable the linearity requirements for maintaining the reliability of the CR receiver for spectrum sensing to be estimated.

***Index Terms*—**Low noise amplifier, IQ imbalance, cognitive radio, nonlinear distortion, software defined radio, direct conversion receiver, wideband transceiver architecture

I. Introduction

The increasing demand for wireless data has motivated the use of CRs to efficiently utilize the available spectrum. CRs use the concept of opportunistic spectrum access which is based on temporal, spatial, and geographic reuse of the licensed spectrum [1]. Software Defined Radio (SDR) has been proposed as one of the possible approaches to opportunistic radio where operating parameters such as frequency range, modulation type, and output power can be adapted by software [2], [3].

Extensive theoretical research on using SDR's in CR-based systems has been conducted. However, system design has been facing many challenges such as the design of frequency agile RF front-ends that can handle the opportunistic spectrum access [3], [4]. In general, since CRs are expected to communicate across a number of frequency channels by continually sensing the spectrum and identifying available channels, multi-channel operation of CR transceivers imposes stringent linearity requirements on the analogue transmit and receive hardware [4]-[9]. Therefore, one of the main challenges in CR receiver design is the co-existence of multiple radio signals which come from different systems [10]-[13]. These RF signals are processed by the RF nonlinearity of Low Noise Amplifiers (LNA) and this results in nonlinear distortion and intermodulation products that lie within the receive bandwidth. The interaction of multiple signals by the nonlinearity results in spectral components that lie in vacant channels (white spaces) or on top of weak signals leading to deterioration of the reliability of the receiver for spectrum sensing. If intermodulation components exist within the white space, the white space is masked reducing the efficiency of the CR system from a spectrum exploitation point of view [6], [10], [14], [17]. Modeling nonlinear distortion in CR receivers, as a result, is important for the proper design of the system in order to mitigate the problem of masking the white spaces and to maintain a proper detection of desired signals in the presence of strong interfering signals.

Another important issue in the design of DCR-based CR receivers is the presence of other types of nonlinearities such as I/Q imbalances and baseband (BB) nonlinearities. The effect of these nonlinearities becomes significant when transmitted signals have high peak-to average power ratio (PAPR) and wide frequency separation [14], [15]. On the other hand, the interaction of these nonlinearities with RF nonlinearities in the receiver chain enhances the intermodulation products which causes further degradation of system performance and results in imposing more stringent linearity requirements on the system.

Several attempts for modeling the combined effect of the various nonlinearities in the receive path in CR receivers have been presented in the literature [14]-[17]. The most relevant study to the current paper is the one in [19]-[22] where the authors studied the effect of I/Q imbalance in DCR-based CR receivers on energy detection (ED)-based spectrum sensing in both single channel and multi-channel scenarios. It was shown that the probability of false alarm in multi-channel energy detection increases significantly as the value of the I/Q imbalance parameters increase.

In [18], the authors studied the effect of intermodulation distortion from a third order LNA nonlinearity on spectrum sensing of DCR-based CR receivers. However, the effects of BB nonlinearities and the IQ imbalance was not considered. The authors of [19]

Manuscript received September 2, 2019; revised March 5, 2020.
doi:10.12720/jcm.15.4.350-358

©2020 Journal of Communications

considered the design of predistortion schemes for wideband receivers to overcome the effects of all types of nonlinearity in the receiver path.

To accurately model the interaction of multiple signals by nonlinearity in DCR-based CR receivers, it is important to develop a generalized model that considers the receiver architecture, the nature of these nonlinearities and their interactions. The objective of this paper is to analyze the interaction of multiple wideband signals at a CR receiver in the presence of RF nonlinearity, BB nonlinearity and I/Q imbalance assuming a generalized *N*-th order of nonlinearity. The significance of the current research is that the model considers the interaction of multiple signals by the three types of nonlinearity in the receiver chain. Thus, the model enables the performance of CR receivers to be realistically assessed for spectrum sensing.

In the following sections, a mathematical formulation of the interaction of multiple signals at a nonlinear CR receiver is presented. The model is then used to predict spectrum sensing capability of the receiver in the presence of the various types of nonlinearity. The analysis is then verified by computer simulations which are used to assess the performance of the receiver at varying parameters of the receiver blocks.

II. Nonlinearity in CR Receivers

Fig. 1 shows a CR wideband transceiver architecture which employs direct conversion to the digital domain [2]. One of the main design challenges in this architecture is the requirement for high dynamic range and high linearity. For the purpose of analyzing nonlinearity in the receiver, a conceptual diagram for the signal path is presented in Fig. 2 [2]. In this diagram, the signal path consists of three main nonlinear impairments: the RF nonlinearity of the LNA, the I/Q imbalance of the mixer and the BB nonlinearity. These nonlinearities represent the main transformations in the receiver path which result in the interaction of the desired signal with interfering signals and causes intermodulation components to mask the white spaces.

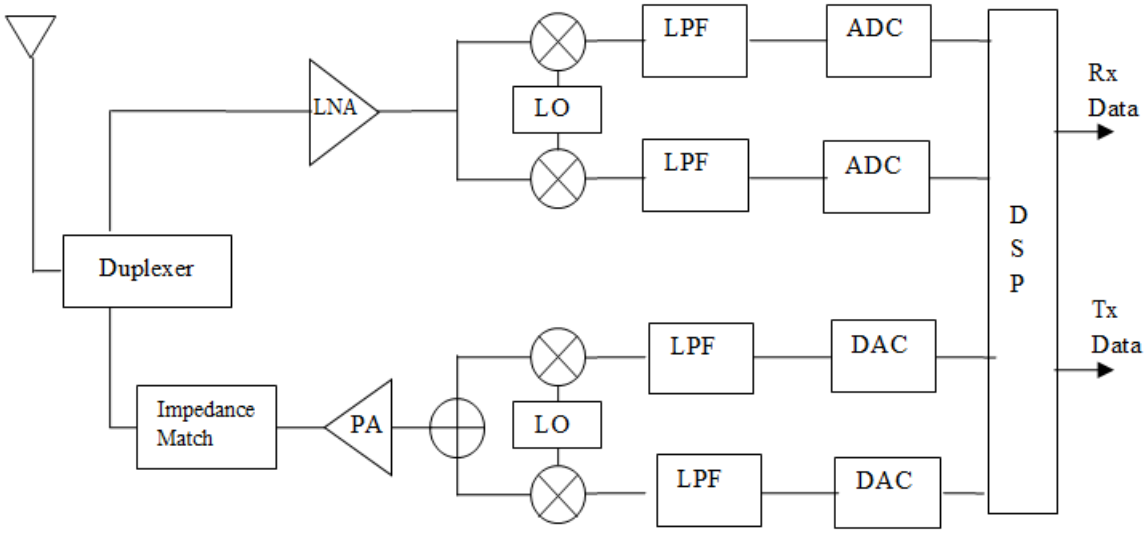

Fig. 1. CR wideband transceiver architectures [2].

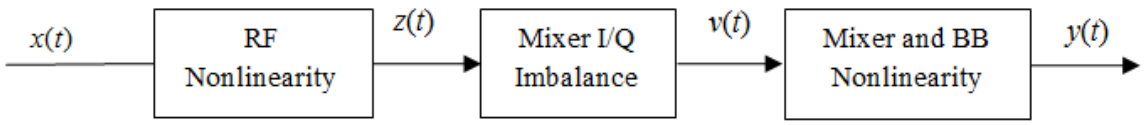

Fig. 2. System model: A cascade of RF nonlinearities, I/Q imbalance and BB nonlinearities [2].

The nonlinearities shown in Fig. 2 are modeled as a cascade of memoryless nonlinearities. The assumption of memoryless nonlinearity is reasonable in the case of wideband receivers and simplifies the analysis as shown in [20]. A further assumption is that these nonlinearities are considered to be pure odd order nonlinearities as even order nonlinearities usually result in intermodulation components which are far away from the desired bands as indicated in [2].

The RF nonlinearity in a CR receiver is manifested by the LNA. The LNA can be modeled as a memoryless nonlinearity of *N*-th order as mentioned in the previous section. Therefore, following Fig. 2, the output of the LNA can be written as

$$z(t) = F_{RF}[x(t)] = \sum_{n=1}^{N} x^n(t) \quad (1)$$

where a_n denotes the *n*-th order coefficient of the memoryless nonlinearity. After amplification by the LNA, the RF signal is down-converted to baseband by the wideband I/Q mixer. Ideally, the down-conversion process results in translating the RF spectrum to BB. However, the imbalance between the amplitude and phase of the *I* and *Q* branches results in compromising the image or mirror frequency attenuation of the analogue front-end [16].

The I/Q imbalance is caused by the relative amplitude mismatch denoted by g_m between I and Q branches as well as their phase mismatch denoted by θ_m. Hence, the output of the I/Q imbalance block in Fig. 2 can be written as [15]:

$$v(t) = k_1\tilde{z}(t) + k_2\tilde{z}^*(t) \quad (2)$$

where $\tilde{z}(t)$ denotes the complex envelope of the input signal to the I/Q imbalance block, * denotes complex conjugation; and k_1 and k_2 denote the complex mismatch coefficients which can be written in terms of the amplitude and phase mismatches as [16]:

$$k_1 = \frac{1}{2}(1+ g_m e^{-j\theta_m}), \quad k_2 = \frac{1}{2}(1+ g_m e^{j\theta_m}) \quad (3)$$

In this model, if the I/Q branches are perfect, then g_m =1 and θ_m = 0 and equivalently: k_1=1 and k_2=0. Typically, wideband receivers can have amplitude and phase mismatches on the order of 1–5% and 1^o –5^o which corresponds to 25-40 dB image attenuation [14]. The output of the I/Q imbalance block can be written as

$$v(t) = v_I(t) + jv_Q(t) \quad (4)$$

where $v_I(t)$ and v_Q are real quantities which can be written using (2) as:

$$v_I(t) = \mathbf{Re}[k_1\tilde{z}(t) + k_2\tilde{z}^*(t)] \quad (5)$$

$$v_Q(t) = \mathbf{Im}[k_1\tilde{z}(t) + k_2\tilde{z}^*(t)] \quad (6)$$

Now considering the BB nonlinearity block in Fig. 2, the output of this block can be written as the complex sum of two nonlinearities of each of the I and Q branches as [15]

$$y(t) = y_I(t) + jy_Q(t) \quad (7)$$

where

$$y_I(t) = F_{BB}^I[v_I(t)] = \sum_{n=1}^{N_{BB}} c_n^I\, v_I^n(t) \quad (8)$$

$$y_Q(t) = F_{BB}^Q[v_Q(t)] = \sum_{n=1}^{N_{BB}} c_n^Q\, v_Q^n(t) \quad (9)$$

where $y_I(t)$ and $y_Q(t)$ represent the I and Q branches at the output of the BB block, F_{BB} represents the BB nonlinear transformation and c_n^I and c_n^Q are the coefficients of the BB nonlinearities of the I and Q branches respectively.

III. Interaction of Multiple Signals by Nonlinearity

In [20], the authors developed a model that enables nonlinear distortion in multi-channel nonlinear power amplifiers to be predicted. In this section, the analysis in [20] will be extended to include the three types of nonlinearity in Fig. 2.

Using the model in (1) and considering an input signal $x(t)$ which consists of the sum of a desired signal $x_1(t)$ centered at frequency f_1 and an interfering signal $x_2(t)$ centered at frequency f_2 such that the input to the nonlinear block is $x(t) = x_1(t) + x_2(t)$, then the complex envelope of the output of the RF nonlinearity at the center frequencies f_1 and f_2 can be written as [20]:

$$z_{f_1(t)} = G_F(r, s, N, \mathbf{a}) \quad (10)$$

$$z_{f_2(t)} = G_F(s, r, N, \mathbf{a}) \quad (11)$$

where r is the complex envelope of $x_1(t)$, s is the complex envelope of $x_2(t)$, $\mathbf{a} = [a_1, a_3, \ldots]$ is the coefficients vector of the memoryless nonlinearity and

$$G_F(r,s,N,\mathbf{a}) = \sum_{n=1}^{N}\sum_{l=0}^{\frac{n-2}{2}} b_{n,l}\,(s^*)^l\,(r^*)^{\frac{n-1}{2}-l}\,(r)^{\frac{n+1}{2}-l}\,(s)^l \quad (12)$$

is the nonlinear gain function at the fundamental and the interfering signals and;

$$b_{n,l} = \frac{a_n}{2^{n-1}}\binom{n}{l, \frac{n-1}{2}-l, \frac{n+1}{2}-l, l}$$

In a similar way to (10) and (11), the intermodulation components at the intermodulation frequencies can be written as [20]:

$$z_{f_1(t)} = G_I(r, s, N, \mathbf{a}) \quad (13)$$

$$z_{f_2(t)} = G_I(s, r, N, \mathbf{a}) \quad (14)$$

where

$$G_I(r,s,N,\mathbf{a}) = \sum_{n=1}^{N}\sum_{l=0}^{\frac{n-2}{2}} b_{n,l}\,(s^*)^{l+1}\,(r^*)^{\frac{n-3}{2}-l}\,(r)^{\frac{n+1}{2}-l}\,(s)^l \quad (15)$$

is the nonlinear gain function at the intermodulation frequency and

$$b_{n,l} = \frac{a_n}{2^{n-1}}\binom{n}{\frac{n-3}{2}-l,\ l+1,\ l,\ \frac{n+1}{2}-l}$$

The above analysis clearly models two main impairments to the performance of the receiver as a result of nonlinear amplification by the LNA: the first is the spectral regrowth and gain compression at the fundamental channels (represented by the nonlinear gain function G_F in (12)) which is responsible of degrading the receiver performance; and the second is the intermodulation spectra (represented by G_I in (15)) which are responsible of masking the white spaces.

Fig. 3 shows a conceptual plot of the response of the LNA to two signals centered at frequencies f_1 and f_2 in the

frequency domain. The figure depicts the two aforementioned impairment to the output spectrum which are the spectral regrowth around the main channels at f_1 and f_2; and the intermodulation components at the intermodulation frequencies $2f_2$-f_1 and $2f_1$+f_1. Note that the power of the intermodulation components depends on the powers of both the desired and interfering signal. Therefore, when the signal power of the main channel at f_1 is low and the power of the interfering channel at f_2 is high, the intermodulation power at the lower intermodulation frequency will be lower than that of the higher intermodulation frequency and vice versa.

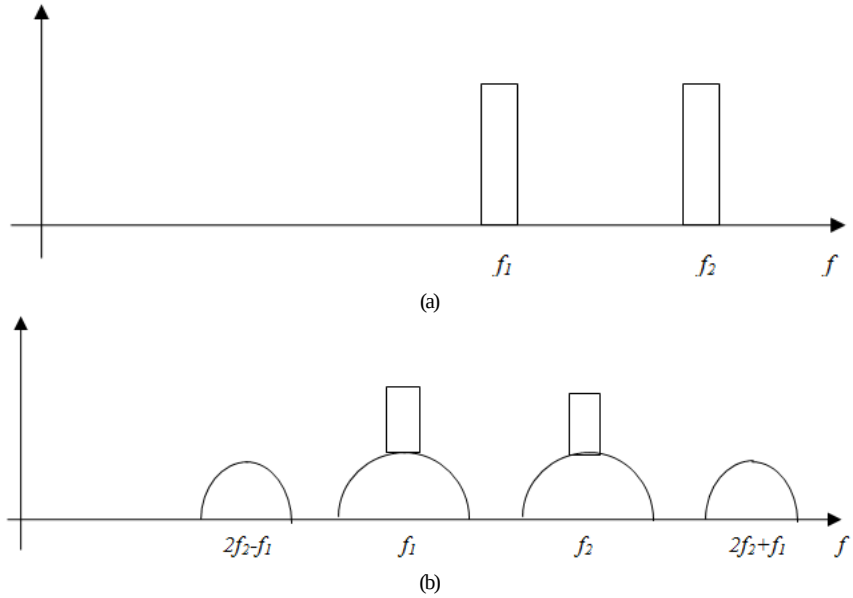

Fig. 3. RF spectra in wideband receiver: (a) Input spectrum of two RF signals to an LNA and (b) Output of RF nonlinearity.

Up to this point, the impact of RF nonlinearity in a CR receiver has been shown to result in intermodulation components that reduce the receiver sensitivity. The effects of the remaining blocks will be studied in order to characterize their combined effect with the RF nonlinearity on the receiver sensitivity.

Assuming that the interfering signal at f_2 and the intermodulation components at $2f_2$-f_1 and $2f_2$+f_1 are removed by RF filtering, so that only the desired signal from the RF block (f_1) is down-converted by the I/Q blocks, the down-conversion process results in a frequency component at the IF frequency and another component at the frequency f_{IF}+(f_2-f_1). In a similar way to the RF stage, the latter can be removed by the IF filtering as shown in Fig. 4a. Therefore, using (5) and (6), the overall output of the I/Q imbalance block can be written as:

$$v(t) = v_{IF} + v_{-IF} \tag{16}$$

where $v_{f_{IF}} = A\tilde{z}_{f_1}(t)$, $v_{-f_{IF}} = B\tilde{z}^*_{f_1}(t)$ and A and B are complex coefficients. Note that the I/Q imbalance results in an attenuated component at the IF frequency represented by $A\tilde{z}_{f_1}(t)$ and an image spectrum at the image frequency f_{-IF} represented by $B\tilde{z}^*_{f_1}(t)$ as shown in Fig. 4b.

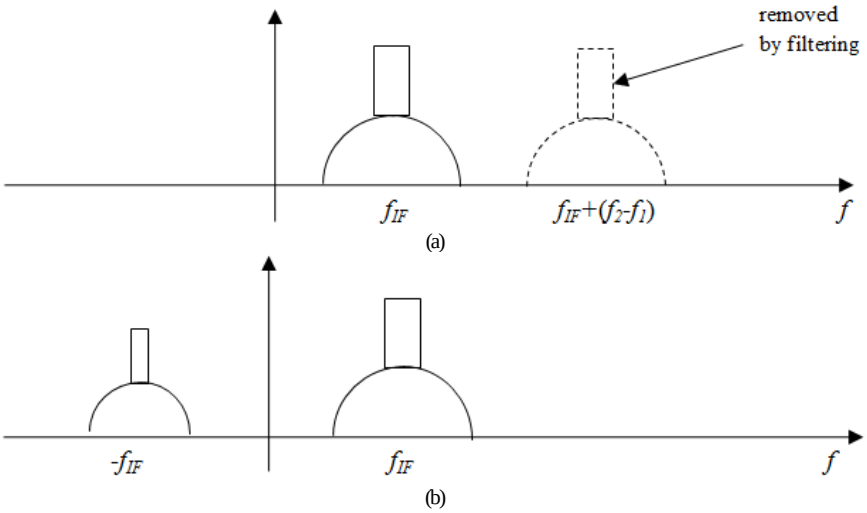

Fig. 4: Spectrum of I/Q down-conversion of an RF signal with I/Q imbalance; (a) input spectrum and (b) the output spectrum.

The output of the BB nonlinearity can now be formulated by inserting (16) into (8) and (9) as:

$$y_I(t) = \sum_{n=1}^{N_B B} c_n^I \left(\mathbf{Re}\left[v_{f_{IF}} + v_{-f_{IF}} \right] \right)^n \quad (17)$$

$$y_Q(t) = \sum_{n=1}^{N_B B} c_n^Q \left(\mathbf{Im}\left[v_{f_{IF}} + v_{-f_{IF}} \right] \right)^n \quad (18)$$

Note that the existence of the spectrum at the image frequency will lead to distortion spectra at multiples of the IF frequency by the BB nonlinearity as shown in Fig. 5b. The figure also shows that the nonlinearities in the receiver chain result in intermodulation spectra that may well interact with the white spaces. In addition, the figure shows the extra spectral regrowth around the desired channel which results from the interaction of multiple signals by the nonlinearity.

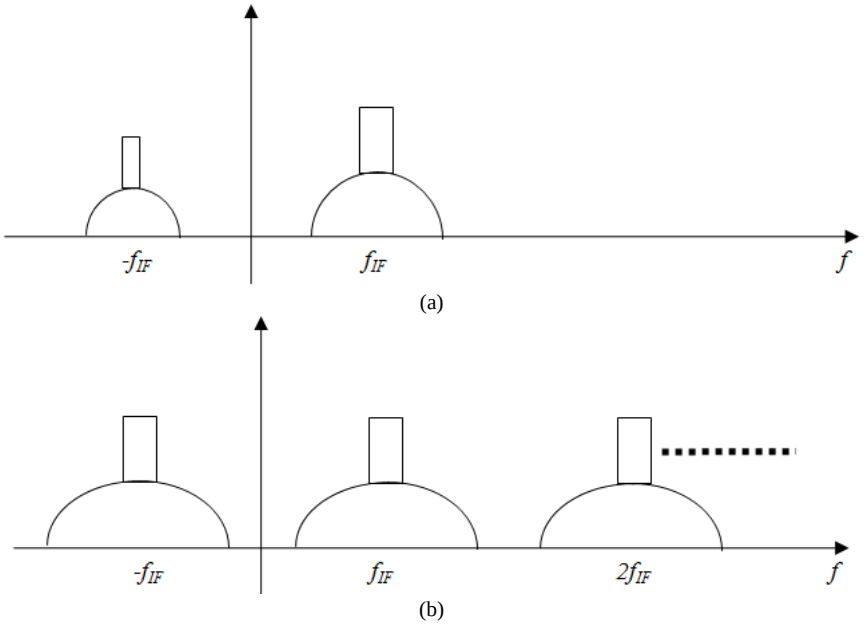

Fig. 5. Spectra of BB nonlinearity: (a) Input spectrum and (b) Output spectrum.

The above development has enabled nonlinear distortion to be evaluated in RF front ends of CR receivers where the effect of strong interferers on the detection of weak signals can be predicted. Similarly, the analysis enables the effect of the combination of interference, BB nonlinearity and I/Q imbalance on the received signal to be predicted. Note that the analysis considers *n*-th order nonlinearities and not just 3rd order nonlinearities as in [15] and [16]. The limitation of the model lies in employing a memoryless nonlinear model. This assumption, although discards memory effects, simplifies the analysis and enables the effects of three types of nonlinearity to be easily modeled and analyzed.

IV. Spectrum Sensing in CR Receivers

Spectrum sensing in CR systems is the process by which the system allows the Secondary Users (SUs) to learn about the radio environment by detecting the presence of the Primary Users (PUs) signals [23]. Several techniques, with different levels of complexity and processing time requirements, have been developed for the purpose of sensing the wide frequency band. By and large,, the spectrum sensing model is formulated as [23]:

$$r(t) = \begin{cases} w(t) & H_0 : \text{PU present} \\ h * s(t) + w(t) & H_1 : \text{PU absent} \end{cases} \quad (19)$$

where $r(t)$ is the SU received signal, $s(t)$ is the PU received signal, $w(t)$ is additive white Gaussian Noise (AWGN) and h represents the channel coefficient.

Since the focus of the current paper is primarily on the effects of nonlinear distortion on the receiver sensitivity, a memoryless linear time invariant channel (h=1) is assumed. Furthermore, the nonlinear distortion $d(t)$ and the AWGN are assumed to be uncorrelated and hence, they can be combined into a single noise component $n(t)=w(t)+d(t)$. Hence, the spectrum sensing model in (19) can be rewritten as

$$r(t) = \begin{cases} n(t) & H_0 : \text{PU Present} \\ hs(t) + n(t) & H_1 : \text{PU Absent} \end{cases} \quad (20)$$

The simplest form of spectrum sensing is the energy detection (ED) technique where the received signal energy is compared to a threshold to detect the existence of a PU.

In this technique, the decision statistic can be modeled as

$$\begin{cases} H_0 & \boldsymbol{E} < \boldsymbol{v} \\ H_1 & \boldsymbol{E} > \boldsymbol{v} \end{cases} \quad (21)$$

where $\boldsymbol{E}$ is the SU signal energy and $\boldsymbol{v}$ is a threshold which can be chosen to be the total noise and distortion variance $\boldsymbol{v} = \sigma_n^2 = \sigma_w^2 + \sigma_d^2$ [24]. The distortion variance

σ_d^2 can be calculated from the PSD of either the upper or the lower intermodulation components in (13) or (14) as

$$\sigma_d^2 = \int_{f_{I-NB}}^{f_{I+NB}} S_{zzI}(f)\,df \tag{22}$$

where f_I is the intermodulation frequency, B is the bandwidth of the PU transmitted signal, and $S_{zzI}(f)$ is the power spectral density (PSD) of the intermodulation signal in (13) or (14). With this assumption, the probability of detection (P_d) and the probability of false alarm (P_{fa}) of the spectrum sensing algorithm can be written as [25]

$$P_d = Q\left(\frac{v-\left(\sigma_t^2+\sigma_s^2\right)}{\sqrt{2\left(\sigma_t^2+\sigma_s^2\right)^2}}\right) \tag{23}$$

$$P_{fa} = Q\left(\frac{v-\sigma_t^2}{\sqrt{2\sigma_t^4}}\right) \tag{24}$$

where $Q(.)$ denotes the Q-function.

TABLE I: ENVELOP POWER SERIES COEFFICIENT

	RF Nonlinearity
b_1	7.63-5.36i
b_3	-56.18+66.95i
b_5	274.24-302.17i
	I/Q Imbalance
g_m	0.9
θ_m	0.25
	BB Nonlinearity
c_I	[1 0 0.5 0 -0.1]
c_Q	[1 0 -0.324 0 0.13]

V. SIMULATION RESULTS AND DISCUSSION

The above analysis of the combined effect of RF, BB and I/Q nonlinearities was implemented in Matlab. These nonlinearities were simulated using the parameters shown in Table I where RF and BB nonlinearities are characterized by power series coefficients. OFDM signals were used as input to the model which were generated according to the specifications in Table II.

TABLE II: SIMULATION PARAMETERS

No. of sub-carriers	1705
Modulation	16 QAM Constellation type: Gray
Pulse Shaping	Rectangular pulse
PAPR	10.8 dB
Input Power range	-30 dBm to -9 dBm

To estimate the PSD's of the output of the cascade, the autocorrelation functions were computed from the time correlation functions of signal realizations and the coefficients of the system model in Table I. Signal realizations of 105 samples were used in the computation of the autocorrelation functions and the power spectra at the output of each of the cascaded blocks in Fig. 2. The PSD's were computed from the Fourier transform of the autocorrelation functions at different input power levels.

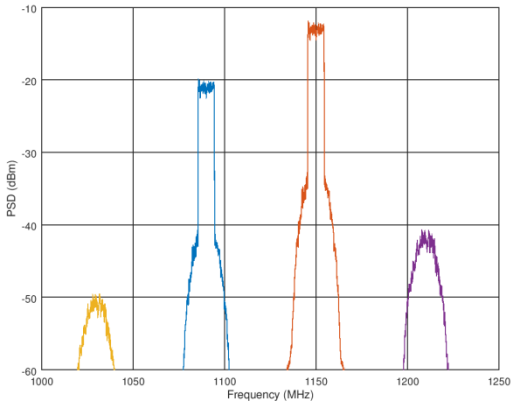

Fig. 6. The output spectrum of the RF nonlinearity for two input signals; Pin1=-18 dBm, Δ: Pin2=-12 dBm.

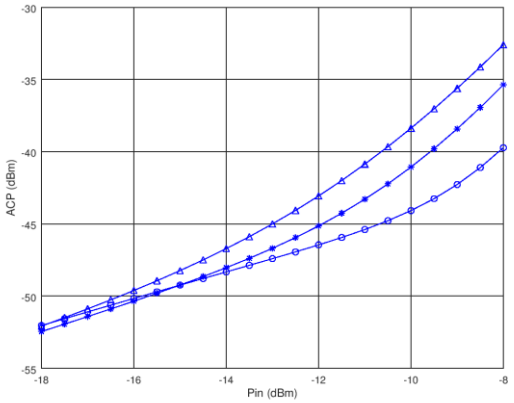

Fig. 7. ACP for various values of input power of the interfering signal; *: Pin_2=-18 dBm, Δ: Pin_2=-12 dBm and o: Pin_2=-10 dBm.

Fig. 6 shows the simulated output spectrum at the output of the RF nonlinearity block for two RF signals at different input power levels. The figure shows the intermodulation components at the intermodulation frequencies which may interfere with the white spaces in a CR spectrum. Fig. 7 shows Adjacent Channel Power (ACP) vs. input power for various power levels of an interfering signal. The figure shows that nonlinear distortion that results from cross modulation between two OFDM signal in a wideband receiver has a significant effect on performance of the system when the interfering signal has comparable power level to the desired signal. The figure shows an increase of about 5 dB in ACP for each 1 dBm of increase in the interfering signal power.

The effect of BB nonlinearity on the received signal was simulated using (16). Fig. 8a shows the spectrum of the desired RF signal after down conversion to an IF frequency of 75 MHz, Fig. 8b shows the spectrum at the output of the I/Q imbalance block and Fig. 8c shows the spectrum at the output of the BB nonlinearity. These figures show how the BB nonlinearity results in extra

spectral regrowth around the spectrum of the desired signal and the spectrum of the image signal which results from the I/Q imbalance.

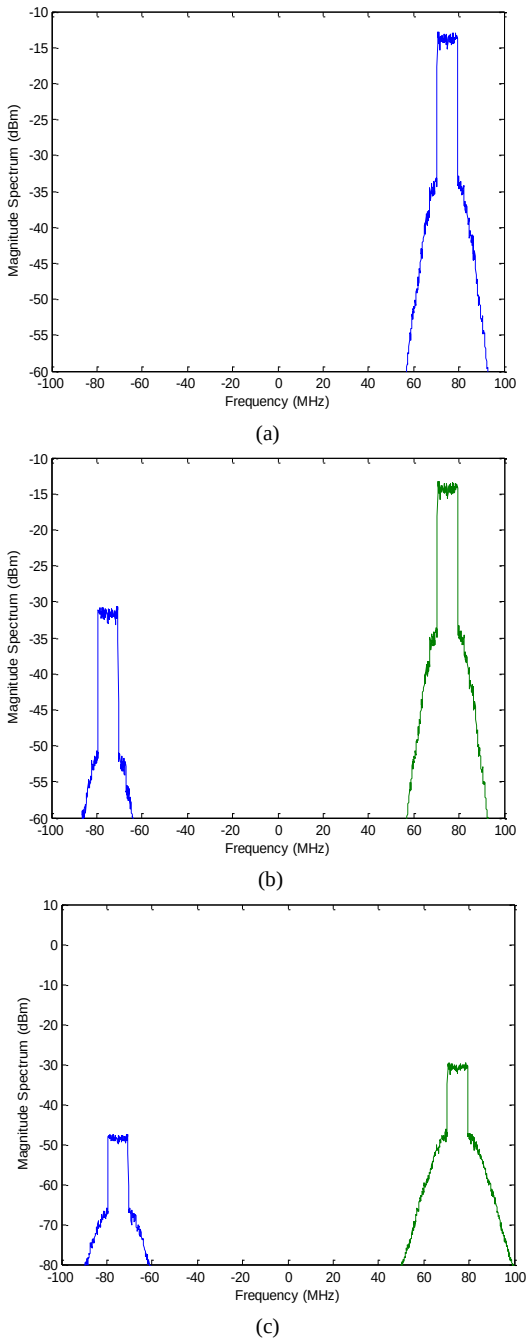

Fig. 8. (a): The output spectrum of the RF nonlinearity after down conversion to IF; (b): The output spectrum of the I/Q imbalance block and (c): The output spectrum of the BB nonlinearity block.

Fig. 9 shows the power spectrum at the output of a cascade of an RF nonlinearity and a BB nonlinearity at an input power of -10 dBm assuming an interfering signal with input power of -12 dBm. The figure shows significant increase in ACP as a result of BB nonlinearity. Fig. 10 shows ACP vs. input power assuming an interfering signal with input power of -10 dBm. The figure shows an increase of up to 30 dB in ACP as a result of the existence of BB nonlinearity.

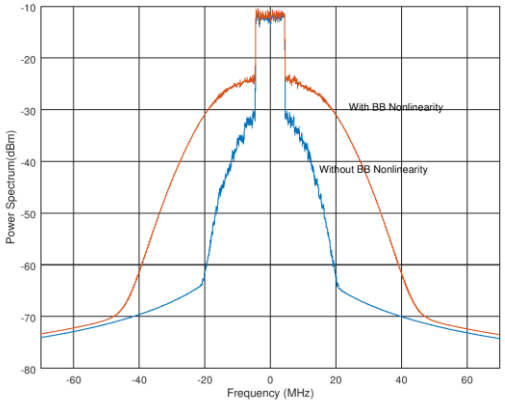

Fig. 9. Power spectrum at the output of the cascade with and without BB nonlinearity.

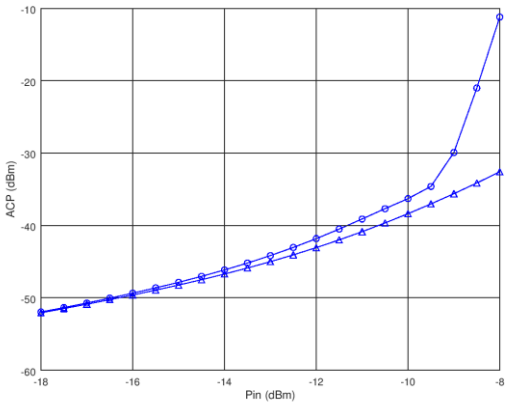

Fig. 10. ACP at Pin2=-10 dBm; Δ: without BB nonlinearity and o: with BB nonlinearity.

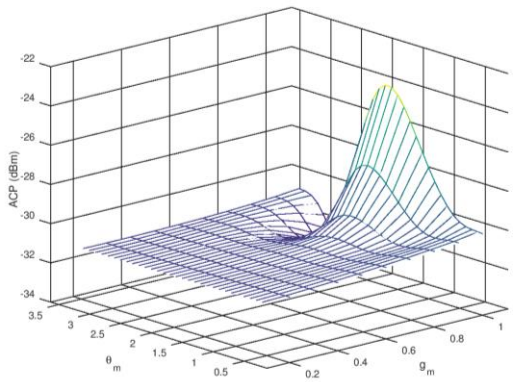

Fig. 11. ACP vs. g_m and θ_m with Pin1= -9 dBm and Pin2=-10 dBm.

Fig. 11 shows a 3-D plot of ACP vs. both I/Q mismatch parameters assuming an input power of -9 dBm and -10 dBm for the desired signal and the interfering signal respectively. The figure further shows that the relationship between the IQ imbalance and ACP is convex indicating the existence of optimal mismatch parameters that result in minimum ACP. The figure also shows that the angle of the I/Q imbalance has a significant effect on the output distortion especially at high input drive levels.

In order to assess the effect of intermodulation products on masking the white spaces, the probability of false alarm was simulated for various values of the input power of the two signals. Fig. 12 depicts the probability of false alarm for a range of values of the input power of the interfering signal. The figure shows that this probability becomes significant when the interfering signal power is increased. The figure can be used for relating the power of the interfering signal directly to probability of masking the white space in CR systems.

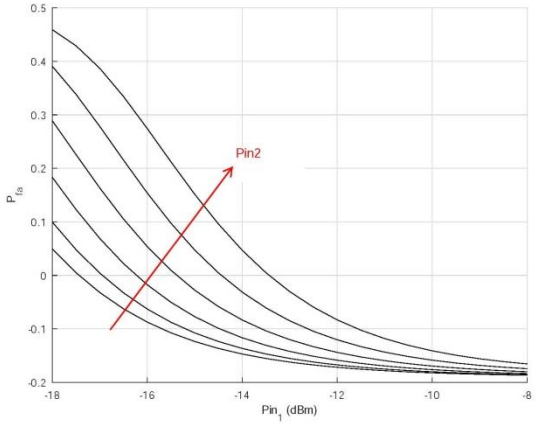

Fig. 12. Pfa vs. Pin1= -9 dBm for Pin2=-20:-10 dBm.

VI. Conclusion

A model for signal interaction by nonlinearity in a wideband receiver of a CR system has been developed. The model considers mixing of two RF signals by an RF nonlinearity and then processing the resulting signal at baseband by the I/Q mismatch and a BB nonlinearity. The computed spectra at the output of the system show that I/Q imbalance and the BB nonlinearity become significant and severely affect the overall performance of the system when an interfering signal exists at the input of the RF nonlinearity. The model also considers the effect of intermodulation components of the two signals on reducing the sensitivity of the CR receiver by masking the white spaces. The model is useful for relating nonlinear distortion to the performance of CR system including the probability of detection and the probability of false alarm.

Conflict of Interest

The author declare no conflict of interest.

References

[1] A. Popescu, "Cognitive radio networks," in *Proc. IEEE 9th International Conference on Communications* (*COMM*), 2012.

[2] V. T. Nguyen, F. Villain, and Y. L. Guillou, "Cognitive radio RF: overview and challenges," *VLSI Design*, p. 1, 2012.

[3] P. Robert and B. A. Fette, "The software defined radio as a platform for cognitive radio," *Cognitive Radio Technology*, pp. 73-118, 2006.

[4] J. Goodman, B. A. Miller, J. Vian, A. Bolstad, A. Kalyanam, and A. Herman, "Physical layer considerations for wideband cognitive radio," in *Proc. Military Communications Conference*, San Jose, CA, Oct. 31-Nov. 3, 2010.

[5] B. Razavi, "Cognitive radio design challenges and techniques," *IEEE Journal of Solid-State Circuits*, vol. 45, pp. 1542-1553, 2010.

[6] S. Dikmese, S. Srinivasan, M. Shaat, F Bader, and M. Renfors, "Spectrum sensing and resource allocation for multicarrier cognitive radio systems under interference and power constraints," *EURASIP Journal on Advances in Signal Processing*, vol. 2014, p. 68, 2014.

[7] A. C. Polak, M. Wagner, M. F. Duarte, R. W. Jackson, and D. L. Goeckel, "Mitigation of spectral leakage for single carrier, block-processing cognitive radio receivers," *Digital Communications and Networks*, vol. 4, pp. 106-110, 2018.

[8] D. H. Mahrof, E. A. Klumperink, J. C. Haartsen, and B. Nauta, "On the effect of spectral location of interferers on linearity requirements for wideband cognitive radio receivers," in *Proc. IEEE Symposium on New Frontiers in Dynamic Spectrum*, Singapore, 2010, pp. 1-9.

[9] M. Renfors, "Cognitive radio and its RF challenges," thesis, Tampere University of Technology, Tampere, Finland, 2009.

[10] P. Kryszkiewicz, H. Bogucka, and A. M. Wyglinski, "Protection of primary users in dynamically varying radio environment: Practical solutions and challenges," *EURASIP Journal on Wireless Communications and Networking*, vol. 2012, p. 23, 2012.

[11] S. Choi, E. Jeong, and Y. H. Lee, "Design of digital predistorters for wideband power amplifiers in communication systems with dynamic spectrum allocation," in *Proc. IEEE International Conference on Acoustics, Speech and Signal Processing*, 2011, pp. 3204--3207

[12] E. Rebeiz, A. S. H. Ghadam, M. Valkama, and D. Cabric, "Suppressing RF front-end nonlinearities in wideband spectrum sensing," in *Proc. International Conference on Cognitive Radio Oriented Wireless Networks*, July 2013, pp. 87-92.

[13] S. Shellhammer, A. K. Sadek, and W. Zhang, "Technical challenges for cognitive radio in the TV white space spectrum," in *Proc. Information Theory and Applications Workshop*, San Diego, CA, 2009.

[14] N. B. Carvalho, A. Cidronali, and R. Gómez-García, *White Space Communication Technologies*, Cambridge University Press, 2014.

[15] M. Valkama L. Anttila, and M. Renfors, "Advanced digital signal processing techniques for compensation of nonlinear distortion in wideband multicarrier radio receivers," *IEEE Transactions on Microwave Theory and Techniques*, vol. 54, pp. 2356-2366, 2006.

[16] M. Grimm, M. Allen, J. Marttila, M. Valkama, and R. Thoma, "Joint mitigation of nonlinear RF and baseband distortions in wideband direct-conversion receivers," *IEEE Transactions on Microwave Theory and Techniques*, vol. 62, pp. 166-182, 2013.

[17] M. Allén, *Nonlinear Distortion in Wideband Radio Receivers and Analog-to-Digital Converters: Modeling and Digital Suppression*, thesis, Tampere University of Technology, Tampere, Finland, 2015.
[18] E. Rebeiz, E. A. S. Ghadam, M. Valkama, and D. Cabric, "Spectrum sensing under RF non-linearities: Performance analysis and DSP-enhanced receivers," *IEEE Transactions on Signal Processing*, vol. 63, pp. 1950-1964, 2015.
[19] J. Marttila, M. Allen, M. Kosunen, K. Stadius, J. Ryynanen, and M. Valkama, "Reference receiver enhanced digital linearization of wideband direct-conversion receivers," *IEEE Transactions on Microwave Theory and Techniques*, vol. 65, pp. 607-620, 2017.
[20] K. M. Gharaibeh and M. B. Steer, "Modeling distortion in multichannel communication systems," *IEEE transactions on Microwave Theory and Techniques*, vol. 53, pp. 1682-1692, 2005.
[21] A. Gokceoglu, S. Dikmese, Sener, M. Valkama, and M. Renfors, "Energy detection under IQ imbalance with single-and multi-channel direct-conversion receiver: Analysis and mitigation," *IEEE Journal on Selected Areas in Communications*, vol. 32, pp. 411-424, 2014.
[22] H. Li and Q. Yiminn, "Effects of IQ imbalance for simultaneous transmit and receive based cognitive anti-jamming receiver," *AEU-International Journal of Electronics and Communications*, vol. 72, pp. 26-32, 2017.
[23] F. Salahdine, "Spectrum sensing techniques for cognitive radio networks," arXiv preprint arXiv:1710.02668, 2017.
[24] M. Subhedar and B. Gajanan, "Spectrum sensing techniques in cognitive radio networks: A survey," *International Journal of Next-Generation Networks*, vol. 3, pp. 37-51, 2011.
[25] D. Bhargavi and C. R. Murthy, "Performance comparison of energy, matched-filter and cyclostationarity-based spectrum sensing," in *Proc. IEEE 11th International Workshop on Signal Processing Advances in Wireless Communications*, 2010, pp. 1-5.

Copyright © 2020 by the authors. This is an open access article distributed under the Creative Commons Attribution License (CC BY-NC-ND 4.0), which permits use, distribution and reproduction in any medium, provided that the article is properly cited, the use is non-commercial and no modifications or adaptations are made.

Khaled M Gharaibeh was born in Irbid, Jordan, in 1972. He received the B.S. and the M.Sc degrees from Jordan University of Science and Technology, Irbid, Jordan, in 1995 and 1998 respectively both in electrical engineering and the Ph.D. degree from North Carolina State University, Raleigh, NC in 2004. He is currently professor of telecommunications engineering at the Applied Science University-Bahrain. His research interests include nonlinear system modeling, wireless communications and wireless sensor networks.